Charles University

Faculty of Science

Study programme: Chemistry

Iryna Morozova

Titration of weak polyelectrolytes in semidilute regime

Titrace slabých polyelektrolytů v polozředěném režimu

Bachelor's thesis

Supervisor: **Ing. Lucie Nová, Ph.D.**

Prague, 2025

Prohlašuji, že jsem závěrečnou práci zpracovala samostatně a že jsem uvedla všechny použité informační zdroje a literaturu. Tato práce ani její podstatná část nebyla předložena k získání jiného nebo stejného akademického titulu. V této práci byla uměla inteligence využita pouze ke zlepšení čitelnosti textu a k opravám jazykových chyb, nikoliv k interpretaci získaných výsledků. Tato práce je zároveň součástí článku "Ionization and chain size of weak polyelectrolytes in semidilute regime" [1].

Praha, 16. 5. 2025 Iryna Morozova

First and foremost, I would like to express my sincere gratitude to my supervisor, Ing. Lucie Nová, Ph.D., for her continuous support, guidance and invaluable feedback throughout my research. Her knowledge and patience greatly enriched this thesis.

I am also thankful to RNDr. Zdeněk Tošner, Ph.D. for introducing me to Nuclear Magnetic Resonance spectroscopy and for generously sharing his expertise and time.

My appreciation also goes to my lab colleagues for the countless discussions, insightful comments and constructive suggestions, which helped me to improve quality of this thesis.

Finally, I am deeply grateful to my family and friends for their unwavering love, encouragement, and sacrifices, without which this journey would not have been possible.

Abstract

This thesis investigates the ionization behaviour of polyacrylic acid, a weak polyelectrolyte, in semi-dilute regime. The primarily focus is on effects of pH and ionic strength on the degree of ionization. Diffusion-Ordered Spectroscopy is employed to determine the overlap concentration (c^*), transition between dilute and semi-dilute regimes. pH titrations are used to analyse how solution's conditions impact degree of ionization. Titration curves obtained from titration experiments, are compared to titration curves obtained from NMR and simulations. Results show that for degree of ionization below 0.8, experimental data are in good agreement with the theoretical model, however, deviations increase at higher degrees of ionization.

Keywords

polyelectrolyte, titration, semi-dilute regime, NMR, DOSY

Abstrakt

Tato práce se zabývá ionizačním chováním polyakrylové kyseliny, slabého polyelektrolytu, v polozředěném režimu. Hlavní pozornost je věnována vlivu pH a iontové síly na stupeň ionizace. K určení překryvové koncentrace (c^*), která představuje přechod mezi zředěným a polozředěným režimem, je využita metoda DOSY. Pomocí pH titrací je analyzováno, jak podmínky roztoku ovlivňují stupeň ionizace. Titrační křivky získané z titračních experimentů jsou porovnávány s křivkami získanými pomocí NMR měření a simulací. Výsledky ukazují, že při stupni ionizace nižším než 0.8 jsou experimentální data v dobré shodě s teoretickým modelem, avšak při vyšších stupních ionizace dochází k rostoucím odchylkám.

Klíčová slova

polyelecktrolyt, titrace, polozředěný režim, NMR, DOSY

List of Abbreviations

PAA	PolyAcrylic Acid
NMR	Nuclear Magnetic Resonance
DOSY	Diffusion Ordered SpectroscopY
DSS	2,2-Dimethyl-2-Silapentane-5-Sulfonate
RAFT	Reversible Addition-Fragmentation chain Transfer
ATRP	Atom Transfer Radical Polymerization
CTA	Chain-Transfer Agent
MW	Molecular Weight
DSTEBP	Double STimulated Echo with BiPolar gradients
PGF	Pulsed-Field Gradient

Contents

1 Introduction

Polymers are large molecules made up of repeating subunits, called monomers, which are connected through chemical bonds. These macromolecules can be divided into natural and synthetic types, both of which are vital in various industries and scientific applications. Natural polymers, such as proteins, DNA, and cellulose, are essential for biological processes and the structural integrity of living organisms. In contrast, synthetic polymers such as polyethylene, polystyrene, and nylon have become a part of our daily lives due to their flexibility, durability, and lightweight properties. The properties of polymers depend on their molecular arrangement, including chain length, branching, and cross-linking, which affect their mechanical durability, elasticity, and thermal stability. These properties make polymers indispensable in various fields including textiles[2], engineering[3], and medicine[4,5].

An important aspect of polymer science is studying polymer solutions. Unlike simple molecular solutions, the polymer dissolution process unfolds gradually through stages of swelling, disentanglement, and the eventual dispersion of polymer chains. The solubility of a polymer in a specific solvent is influenced by multiple factors, such as molecular weight, temperature, and the intermolecular interactions between polymer and solvent molecules. The distinct behaviour of polymer solutions stems from the significant size and complex interactions of polymer chains, which greatly affect their physical and chemical properties.

The characteristics of polymer solutions are significantly influenced by factors such as concentration, solvent quality, and temperature. At low concentrations, polymer chains exist discretely in the solution, while at higher concentrations, they overlap, forming entangled networks that affect viscosity and flow behaviour. The way polymer chains interact with solvent molecules also determines whether a polymer takes on an expanded shape (in good solvents) or collapses into compact configurations (in poor solvents)[6]. Solvents are commonly classified in three groups: good, poor or theta. In good solvents, polymer-solvent interactions are more favourable than the polymer-polymer interactions. In contrast, poor solvents favour polymer-polymer interactions, causing polymer chains to collapse. Theta solvents represent special case in which all the interactions mentioned above are balanced, and the polymer behaves as an ideal coil.

Polyelectrolytes are polymers that, among other groups, consist of ionizable groups, meaning that they can dissociate in aqueous solutions to form charged macromolecules. Based on the ionizable group we can separate polyelectrolytes into two groups - weak and strong polyelectrolytes. While strong polyelectrolytes ionize completely in a solution, weak polyelectrolytes ionize only partially.

Polyacrylic acid is water-soluble anionic (negatively charged) polyelectrolyte. PAA consists of carboxyl functional groups, making it highly sensitive to pH changes.

pH measurement is one of the most commonly used methods for studying ionization processes. It provides valuable information about the degree of ionization and the acid-base behaviour of substances in solution. Titration is a commonly used method when talking about pH changes. Titration curve of a strong electrolyte, for example, typically exhibits a sigmoid shape. In contrast, titration curve of more complex systems, like polyelectrolytes, can deviate significantly from this shape. This deviation is largely influenced by the solution's ionic strength, which affects the electrostatic interactions and the activity of ions in the system. Therefore, understanding the role of ionic strength is essential when analysing the behaviour of weak electrolytes and polyelectrolytes during titration.

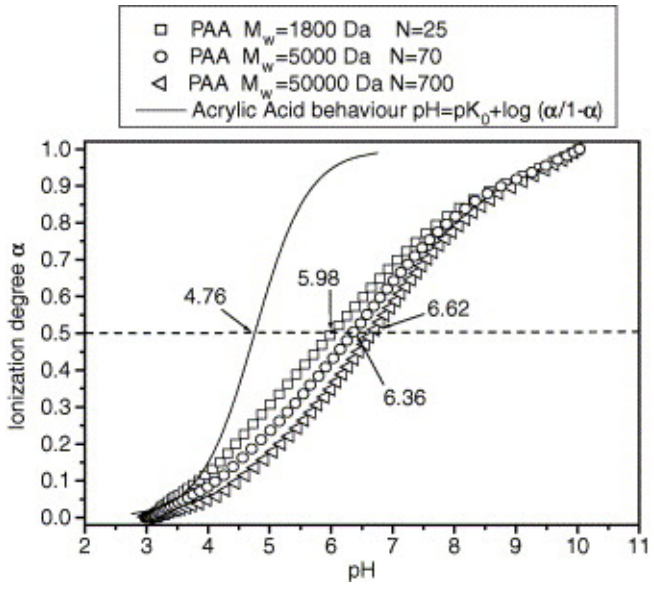

Figure 1: Titration curves of polyacrylic acid with different chain length in comparison with acrylic acid[7]

The aim of this thesis is to investigate how external conditions, such as pH and ionic strength, influence the behaviour and ionization of PAA in the semi-dilute regime.

2 Theoretical part

2.1 Polymer solutions

Polymers in solution exhibit distinct behaviour depending on their concentration. This behaviour arise due to how polymer chains interact with each other and the solvent. As the concentration of polymer increases, the solution passes through different regimes: dilute, semi-dilute, and concentrated. Each regime has unique physicochemical properties that depend on the polymer structure and interactions of the polymer chains[8].

In the dilute regime, polymer coils are sufficiently separated such that they do not overlap or interfere with one another. Each polymer chain behaves independently, occupying its own volume. The conformation of each chain results from a balance between thermal fluctuations and solvent-polymer interactions. The size of a polymer coil is strongly influenced by the solvent quality and the nature of excluded volume interactions. In a good solvent, strong polymer-solvent interactions cause the chain to swell, leading to a radius of gyration scaling as $R_g \sim N^{0.588}$. In contrast, in a theta solvent, where attractive and repulsive interactions cancel on average, the polymer behaves like an ideal Gaussian chain with $R_g \sim N^{0.5}$. These scaling laws are fundamental in polymer physics, confirmed by a wide range of experiments, simulations, and theoretical models[6,8–10]. The radius of gyration serves as representative example of how polymer size depends on chain length and solvent quality, and was not measured in this thesis.

Overlap concentration, usually marked as $c*$, is a critical concentration at which occurs the transition from the dilute to semi-dilute regime. The average distance between polymer chains becomes comparable to the size of an individual coil. The overlap concentration can be described as

$$c^* \sim \frac{Nb^3}{R^3}, \tag{1}$$

where N is degree of polymerization, b is statistical segment length, and R is the size of a chain. This relation reflects the condition that the volume occupied by the polymer segments at the overlap concentration is comparable to the polymer coil's volume itself[6].

Above c^*, the solution enters into what is known as the semi-dilute unentangled regime. In this regime, polymer chains start to overlap, yet avoiding topological entanglements.

The solution exhibits viscoelastic behaviour, demonstrating both liquid-like and solid-like properties due to hydrodynamic interactions, although these interactions are not strong enough to significantly restrict chain mobility[6].

In the semi-dilute unentangled regime scaling laws become particularly important for characterizing polymer solution properties. Solution viscosity follows power-law dependency on concentration. For example, specific viscosity scales approximately as $\eta_{sp} \sim c^{0.51}$, illustrating the resistance in movement of chains due to their overlapping interactions[9,11]. Although viscosity was not measured in this thesis, it serves as a representative example of how polymer solution's properties can change abruptly during regime transitions.

A key characteristic of semi-dilute regime is the correlation length, ξ, representing the average distance over which polymer chains exhibit correlated fluctuations[12]. This means that at distance $r < \xi$ the segments experience excluded-volume interactions, resulting in non-ideal chain conformations. However, at distance $r > \xi$ the dense network of overlapping chains screens those interactions and the chain follows ideal (Gaussian) statistics[9]. As polymer concentration increases, the correlation length decreases, indicating more denser polymer network.

As the concentration increases, the solution reaches entanglement concentration (c_e), where chains are sufficiently overlapped and begin to form a network of entanglements. This denotes the transition to semi-dilute entangled regime. Here, the motion of each polymer chain is significantly restricted by neighbouring chains. Specific viscosity follows relation

$$\eta_{sp} \sim c^{2.56} \tag{2}$$

Specific viscosity increases more steeply with concentration compared to unentangled regime[11]. As the result, mechanical and rheological properties change dramatically.

In the concentrated regime ($c > c^{**}$), polymer chains are densely packed, which means that their motion is highly restricted. Solution behaves more like a transient network, leading to higher viscosity compared to semi-dilute regime. Correlation length decreases to nanometre scale.

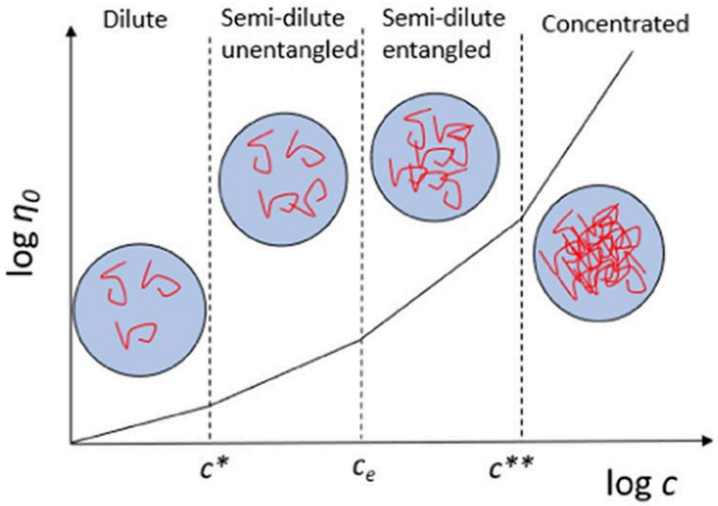

Figure 2: Concentration regimes of polymer solutions[13]

2.1.1 Polyacrylic acid

Polyacrylic acid (PAA) is a synthetic water-soluble polymer derived from the polymerization of acrylic acid monomers. It exhibits a range of distinctive physicochemical properties, such as pH sensitivity, high water absorption capacity and polyelectrolyte behaviour, making it a versatile material across diverse industries: from biomedical engineering to personal care[14].

The structure of PAA consists of repeating acrylic acid units, with general formula $-[CH_2-CH(COOH)]_n-$. PAA is primarily synthesized via free radical polymerization of acrylic acid. Initiators such as potassium persulfate or benzoyl peroxide are commonly used[15]. While conventional free radical polymerization is widely used for its simplicity, advanced polymerization techniques like RAFT and ATRP offer greater control over molecular weight distribution and enable to achieve polymer with defined architecture. In this work, the synthesis of PAA was not performed and is discussed here solely for informational purposes.

Molecular weight significantly influences its behaviour and application. Low molecular weight ($M_w < 20$kDa) PAA behaves as simple anionic polyelectrolyte that can be absorb on mineral or pigment surfaces and are sold as high-efficiency scale inhibitor or dispersant additives such as at ACUMER™ 1000 Polymer. In contrast, high molecular weight PAA, when lightly cross-linked, swell into super-absorbent hydrogel that can hold hundreds of times their own mass (Carbopol®). Molecular weight can be controlled through initiator

concentration, temperature, reaction time and CTAs. For example, by increasing initiator concentration more short radical chains will be formed[16].

One of the key features of PAA is its solubility in water and pH-responsiveness. The carboxylic groups ionize in aqueous solution under basic conditions, forming negatively charged carboxylate ions. The ionization induces electrostatic repulsion between polymer chains, causing them to swell. In contrast, in acidic conditions, carboxylic groups become protonated, minimizing repulsion, which leads to polymer chain collapse.

As a weak polyelectrolyte, PAA's behaviour depends on environmental conditions such as pH, ionic strength and temperature. In ionized state, PAA forms extended coils due to intra- and inter-chain electrostatic repulsion. This results in a characteristic rheological property as shear thinning.

PAA demonstrates moderate thermal stability, with decomposition beginning typically above 175°C[17]. Its mechanical properties depend on molecular weight, degree of cross-linking, or ambient humidity. In aqueous solutions, PAA behaves as viscoelastic fluid, whereas cross-linked PAA can exhibit elastic or plastic behaviour.

PAA is a multifunctional polymer used in wide range of fields. For instance, low M_{w} PAA can be used as general purpose water treatment antiscalant (Aquatreat®AR 901). In biomedicine, PAA hydrogels exhibit a sharp swelling transition around pH 5-7, allowing them to protect active compounds in the acidic environment of the stomach and release them in the intestine or tumour environment, making PAA a key material in modern hydrogel-based drug-delivery systems[18].

2.2 Titration

Titration is a fundamental technique used in analytical chemistry to determine the precise concentration of the analyte in a sample. The procedure involves gradual addition of titrant, a solution of known concentration, into the analyte until it reaches the equivalence point, where the titrant and analyte have reacted in exact stoichiometric amount.

Since the equivalence point is a theoretical concept, it cannot be measured directly. Instead, it is typically approximated by detecting a physical change, such as colour change or change in response of an instrument, that signals chemical equivalence. This observed

change occurs in what is known as the end point[19].

Indicators are chemical substances often used in titration to signal the end point. An ideal indicator changes colour as close as possible to the actual equivalence point. Common indicators are phenolphthalein and methyl orange. In some titrations, self-indicating titrants like potassium permanganate are used.

One of the strengths of titration lies in its accuracy and simplicity. It is widely used in various fields such as pharmaceutical, environmental, food analysis and industrial[20].

2.2.1 pH of a weak polyelectrolyte

pH scale gives us the acidity or alkalinity of solutions, defined as negative logarithm of activity of hydrogen ions

$$\mathrm{pH} = -\log_{10}(a_{\mathrm{H}^+}) \tag{3}$$

Activity refers to the effective concentration of species in solution and is defined as

$$a = \gamma \cdot c, \tag{4}$$

where γ is activity coefficient. The activity coefficient is usually assumed to be approximately equal to 1, $\gamma \approx 1$, which result in the approximation

$$\mathrm{pH} \approx -\log[\mathrm{H}^+], \tag{5}$$

where $[\mathrm{H}^+]$ is hydrogen ion concentration. On pH scale values below 7 indicate acidic solutions, pH = 7 is neutral (pure water at 25°C) and values above 7 indicate alkaline solutions. The pH scale typically ranges from 0 to 14, but negative pH and pH above 14 can occur in highly concentrated solutions.

Strong electrolytes, such as strong acids (HCl) or strong bases (NaOH), dissociate completely in aqueous solutions. This means, that the concentration of hydrogen ions or hydroxide ions is directly proportional to the initial concentration of the acid or base.

In contrast, weak electrolytes, such as weak acids (CH_3COOH) or weak bases (NH_3), dissociate partially in aqueous solutions. Equilibrium between the dissociated and undissociated forms depends on the equilibrium constant (K_a for acids and K_b for bases). The

resulting pH depends not only on initial concentration but also on the strength (degree of ionization) of weak electrolyte.

$$\mathrm{pH} - \mathrm{p}K_\mathrm{a} = -\log\frac{1-\alpha}{\alpha} \tag{6}$$

This equation is known as Henderson-Hasselbalch equation.

Ionic strength defines total ion concentration in solution and can be mathematically expressed as

$$I = \frac{1}{2}\sum_{i=1}^{n} c_i z_i^2, \tag{7}$$

where c_i is molar concentration of ions i and z_i is charge of ion i.

Weak polyelectrolytes, like PAA, possess multiple ionizable groups. Their dissociation depends heavily on hydrogen ion activity and intramolecular electrostatic interactions, creating complex equilibrium that differs significantly from simpler electrolyte solutions.

Calculating pH of weak polyelectrolyte is challenging due to multiple ionizable groups. This means we should account ionic strength and local electrostatic interactions. One comprehensive approach to describe these interactions is represented by

$$\mathrm{pH} - \mathrm{p}K_\mathrm{a} = k \cdot \alpha - \log\frac{1-\alpha}{\alpha} + k_\gamma \frac{A|z^+ z^-|\sqrt{I}}{1 + B \cdot r \cdot \sqrt{I}}, \tag{8}$$

where k and k_γ are adjustable parameters, $A = 0.5085$ mol$^{-1/2}$dm$^{3/2}$ and $B = 0.3281 \times 10^{-8}$ cm^{-1}mol$^{-1/2}$dm$^{3/2}$ are constants, $r = 9$ Å is the distance of closest approach of ions. The final term in Equation (8) serves as the correction for non-ideality, specifically accounting electrostatic interactions between charged species.

2.2.2 Potentiometric titration

Potentiometric titration using titrator is modern analytical technique in which titrator is used to add titrant to a sample solution while measuring the change in electrical potential. Unlike manual titrations, titrator allows to reach high precision and reproducibility.

The principle of potentiometric titration lies in monitoring the potential of an electrode as a function of volume of the titrant. The resulting plot of potential (pH) versus added

volume forms sigmoid curve where the inflection indicates the equivalence point.

An automatic titrator usually consists of titrant reservoir with dosing system, titration vessel, stirrer, pH electrode, thermometer and computer with analysis software.

Before performing a potentiometric titration, the electrode should be calibrated. Calibration is a critical step here because it ensures that the electrode provides accurate and reproducible measurements. Since the end point relies on the potential measured by electrode, any drift or inaccuracy can lead to a significant errors. Calibration is typically performed in two or three standard buffer solutions (e.g., pH 4.00, 7.00 and 10.00) depending on pH range of interest. There are two key calibration criteria. The first one is slope. A slope between 95% and 105% of the ideal Nernst slope, which approximately equals to 59.16 mV/pH at 25°C, is generally acceptable. The second criteria is offset, also known as zero potential, which is measured potential in a neutral buffer solution. The ideal offset is 0 mV, but value within ± 30 mV is considered acceptable.

Automatic titrators offer several advantages over manual titration. They enhance precision, reduce operator variability and are well-suited for experiments with minimal supervision. The equivalence point is determined by analysing the rate of pH change, often using mathematical methods such as first derivative of the curve.

Despite their advantages, automatic titrators require regular maintenance, proper calibration and training to operate correctly. Errors can arise if electrode is not properly cleaned, if titrant solution is not correctly standardized or if the software parameters are improperly configured.

2.2.3 Limitations of pH measurements

Several factors can affect accuracy and reliability of the measurement [19].

1. Calibration error

Improper or infrequent calibration of pH electrode can result in systematic measurement errors. This may occur due to outdated buffers, temperature mismatch or incorrect calibration procedure, leading to inaccurate slope or offset value.

2. The alkaline and acid error

At extreme pH, especially above 12 (alkaline error) or below 1 (acid error), the electrode may deviate from normal behaviour. This occurs due to electrode reacting to other ions, causing a drift in measured pH.

3. Dehydration

Glass electrode depends on a hydrated layer for ion exchange. If electrode dries out due to improper storage or prolonged use in non-aqueous solutions, the response becomes inaccurate.

4. Viscosity of the solution

Highly viscous samples can hinder the diffusion of hydrogen ions to the electrode surface, leading to slow response time and unreliable readings.

2.3 Nuclear Magnetic Resonance

Nuclear Magnetic Resonance (NMR) is nondestructive analytical technique used in chemistry, physics and medicine, to study the properties of atomic nuclei. It is based on the property of many nuclei called spin. The spin generates magnetic moment, and this results in them behaving like tiny magnets. When placed in a strong external magnetic field, it forces nuclei to align with or against this magnetic field, resulting in different energy states. This means that the energy absorbed or emitted by these nuclei varies according to their chemical origin. By analysing nuclei response to magnetic field, we can obtain precious information about structure, dynamics and interactions of molecules[21].

2.3.1 Principles of NMR spectroscopy

The core quantum principle of NMR is that many nuclei possess an intrinsic angular momentum called spin, which is characterized by the quantum number I. This number may only be integer or half-integer. Nuclei with $I \neq 0$ are NMR-active, while those $I = 0$ are NMR-silent. For given nucleus the number of distinct magnetic orientations available in a static field is $2I + 1$.

Every molecule with non-zero spin has magnetic moment, μ. The magnetic moment operator $\hat{\mu}$ is directly proportional to its spin angular momentum operator $\hat{I}$. The relation

is

$$\hat{\mu} = \gamma \hbar \hat{I}, \tag{9}$$

where γ is gyromagnetic ratio and $\hbar$ is reduced Planck constant[22].

Each isotope has a unique γ value. A large γ as in ^{1}H or ^{19}F means that they generate strong magnetic field and therefore produce robust NMR signal. Isotopes with small γ, like ^{15}N, are far less sensitive. In NMR, γ serves as 'sensitivity index'.

When external magnetic field B_0 is applied, magnetic field interact with magnetic moment of atom's nucleus. The magnetic field influences the energy levels of different nuclei unequally, leading to separation of spectral lines. This is known as Zeeman's effect. The separation is always proportional to gyromagnetic ratio and to magnetic field's strength.

In the presence of external magnetic field, nuclei exhibit precessing motion around the direction of magnetic field. This motion occurs at specific frequency called Larmor frequency which is unique to each nucleus. Larmor frequency is measured during NMR experiment and is defined as

$$\nu = \gamma \cdot B_0 \tag{10}$$

When individual magnetic moments of nuclei in a sample combine, they produce what is known as net magnetization vector. Since magnetic moments are vectors, which are aligned randomly, the net magnetization of a sample is zero. However, when external magnetic field is applied to the sample, the net magnetization aligns with the direction of applied field[23].

2.3.2 Chemical shift

Chemical shift is core value reported in NMR spectra. It measures how far the resonance frequency of a given nucleus is displaced from reference compound. Because chemical shift is given as ratio (ppm, parts per million) rather than an absolute frequency in Hertz, spectra collected at different magnetic field strengths are directly comparable. For instance, a signal at 1.000 ppm on a 300 MHz spectrometer will also appear at 1.000 ppm on an 800 MHz spectrometer.

Chemical shift of nucleus, δ, is defined as

$$\delta = 10^6(\frac{\nu - \nu_{ref}}{\nu_{ref}}), \tag{11}$$

where ν is the frequency of nucleus and ν_{ref} is the frequency of a standard.

As reference compound, for organic solvents is usually used TMS, while for aqueous solution DSS is used. Reference compound gives one signal, which is singlet, at 0 ppm. But, all other protons in DSS give minor peaks at around 2.91 ppm, 1.75 ppm and 0.63 ppm with total intensity 22% of the main signal, so they rarely interfere with analyte's spectra.

2.3.3 Solvent suppression

In NMR experiments it is often necessary to use solvent that also contains nuclei of the type being observed[23]. To solve this issue, solvent suppression techniques have been developed to reduce or eliminate solvent peak intensities, thereby enhancing the visibility of solute signals.

Presaturation is one of the simplest and most widely used techniques. It involves application of soft pulse at the resonance frequency of solvent. This pulse saturates solvent magnetization, resulting in significant reduction of solvent signal in spectrum. However, presaturation can affect nearby resonances and is best suited for cases where the solvent peak does not overlap with analyte signals.

2.3.4 Pulse experiments

In ^{1}H pulse experiments, short pulses are used to turn net magnetization from z-axis into transverse xy-plane, initiating free induction decay (FID), which is then detected[24].

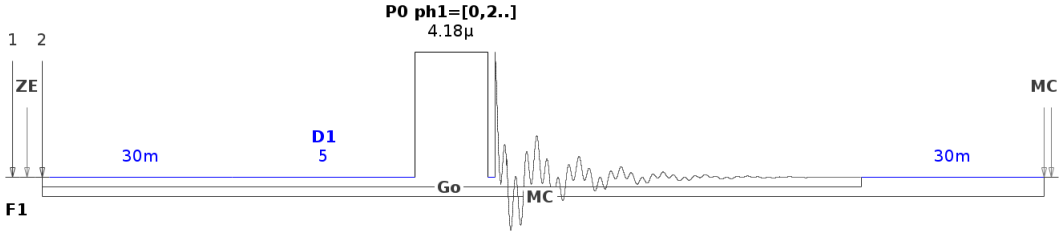

Figure 3: ^{1}H pulse program

In ^{13}C pulse experiments, similar principle applies, but challenges arise due to the low natural abundance (1.1%) and lower sensitivity of ^{13}C isotope. This necessitates longer acquisition times or use of signal enhancement techniques such as proton decoupling[24].

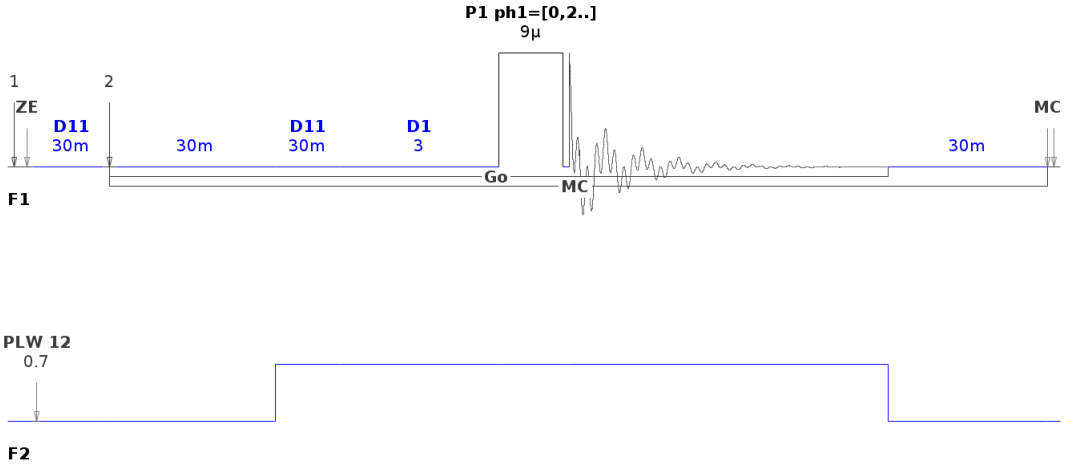

Figure 4: ^{13}C pulse program

2.3.5 DOSY

Diffusion-ordered spectroscopy (DOSY) is advanced NMR technique that provides insight into the diffusion behaviour of molecules in solution. Unlike traditional NMR, which primarily focuses on chemical shifts, DOSY helps to separate molecules based on their translational diffusion coefficients.

The fundamental principle of DOSY lies in the fact that different molecules diffuse with different rates based on their size, shape and interaction with the solvent. In a typical DOSY experiment, a spin echo spectrum is recorded with varied pulsed field gradient strengths. As the gradient strength increases, molecules that diffuse more rapidly have more pronounced attenuation of their signals[25].

Double stimulated echo with bipolar gradients (DSTEBP) is an extension of the standard DOSY which allows to achieve more reliable results[26].

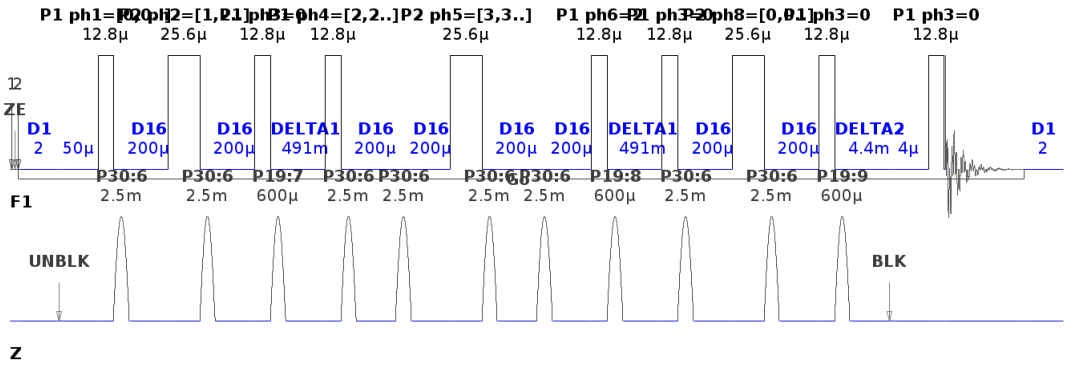

Figure 5: DOSY pulse program

In DOSY, signal attenuation due to molecular diffusion at different pulsed field gradient strengths is a key measurable parameter. The intensity of NMR signal decreases and this decay can be modelled to extract diffusion coefficients. Sometimes, for polymer solutions signal attenuation cannot be described by a single diffusion coefficient. Instead, in this thesis, bi-exponential model is used

$$I(x) = a \cdot e^{-kx^2\delta^2(\Delta-\frac{\delta}{3})\cdot D_1} + b \cdot e^{-kx^2\delta^2(\Delta-\frac{\delta}{3})\cdot D_2}, \tag{12}$$

where a and b are relative contributions of the two exponential components, D_1 and D_2 are translation diffusion coefficients, Δ is diffusion delay, δ is time during which the gradients were switched on (PFG duration), x is gradient strength and k is experimentally determined constant, which was calibrated using water solution with well-known diffusion coefficient.

2.3.6 Applications

NMR is widely used in organic chemistry for determination of unknown substances, for verification of synthesized compounds and for investigation of reaction mechanisms.

Beyond chemistry, NMR has significant application in medicine, known as Magnetic Resonance Imaging (MRI). By detecting the difference in concentration and relaxation properties of water molecules in various tissues, it generates high-resolution images of soft tissues

3 Experimental part

3.1 Chemicals and instrumentation

Titrator	Metrohm 888 Titrando
Electrode	Metrohm LL Biotrode 3mm WOC
NMR spectrometer	Bruker Avance III HD 600 MHz
1M NaOH	Carl Roth GmbH & Co. Kg
5M NaOH	VWR International
Poly(acrylic acid), 25 wt% soln. in water (M_W = 240 kDa)	Thermo Fisher Scientific Inc
pH buffer solution ROTILABO® pH 4.01 in sachets	Carl Roth GmbH & Co. Kg
pH buffer solution ROTILABO® pH 7.00 in sachets	Carl Roth GmbH & Co. Kg
pH buffer solution ROTILABO® pH 10.01 in sachets	Carl Roth GmbH & Co. Kg
Ultrapure water	Milli-Q®

3.2 Nuclear Magnetic Resonance

Each sample was prepared as follows. PAA was first weighed into a vial, then diluted with ultrapure water. A measured volume of NaOH solution was added until the required degree of neutralization (α) was reached. About 0.5 mL of sample was transferred to an NMR tube. Finally, internal standard in special inner tube containing D_2O and traces of DSS was inserted.

One-dimensional ^1H and ^{13}C NMR spectra were acquired on a Bruker Avance III spectrometer operating at proton Larmor frequency of 600 MHz and equipped with standard 5 mm BBO probe. The values of chemical shift were evaluated as the centre of mass of carbonyl region.

Translation diffusion coefficients were measured using DSTEBP pulse sequence[26] with 32 gradient steps with gradient strength incrementing from 5% to 98% of the maximum value (50 G cm^{-1}). Gradient pulses of 2.5 ms duration were separated by a diffusion

delay of 1 s. The absolute diffusion coefficients were calibrated by setting the diffusion coefficient of the residual HDO signal to 1.90 $\times 10^{-9}$ m^2 s^{-1} at 25°C[27]. All spectra were processed in TopSpin 3.6 (Bruker), and the DOSY intensity decays were fitted in Origin using Stejskal-Tanner Eq. (12).

3.2.1 ^{1}H spectra

Figure 6 shows the ^{1}H spectrum of 1.575M solution of PAA at degree of ionization 0.380. A highly intense peak is observed at around 5 ppm, which corresponds to the solvent signal (water). Broad resonance at around 2 ppm arises from hydrogens along the polymer backbone. A sharp singlet at 0.00 ppm originates from DSS, which is used here as an internal standard for chemical referencing.

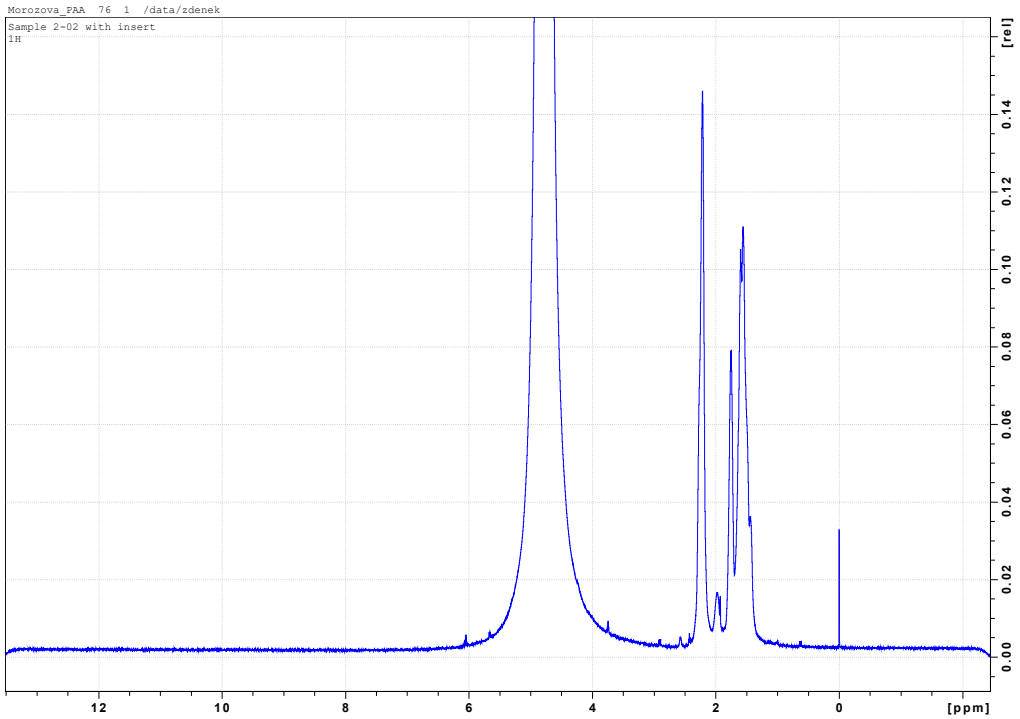

Figure 6: ^{1}H spectrum of 1.575M solution at $\alpha = 0.380$

Figure 7 shows the ^{1}H spectra of 0.4M solutions of PAA at different degrees of ionization. Blue corresponds to $\alpha = 0.207$, red to $\alpha = 0.725$ and green to $\alpha = 0.996$. As degree of ionization increases, chemical shift decays, indicating increased shielding. This effect is likely due to deprotonation of carboxylic groups. Additionally, ionization may alter the polymer's conformation or solvation shell, further modifying the magnetic environment.

In almost non-ionized state, spectrum has sharper, more defined peaks. As ionization increases, broadening begins due to electrostatic interactions. In fully ionized state, broadest signals with reduced fine structure are observed due to ion-ion and solvent-ion interactions.

The appearance of a triplet in fully ionized spectrum is likely attributed to reduced conformational averaging.

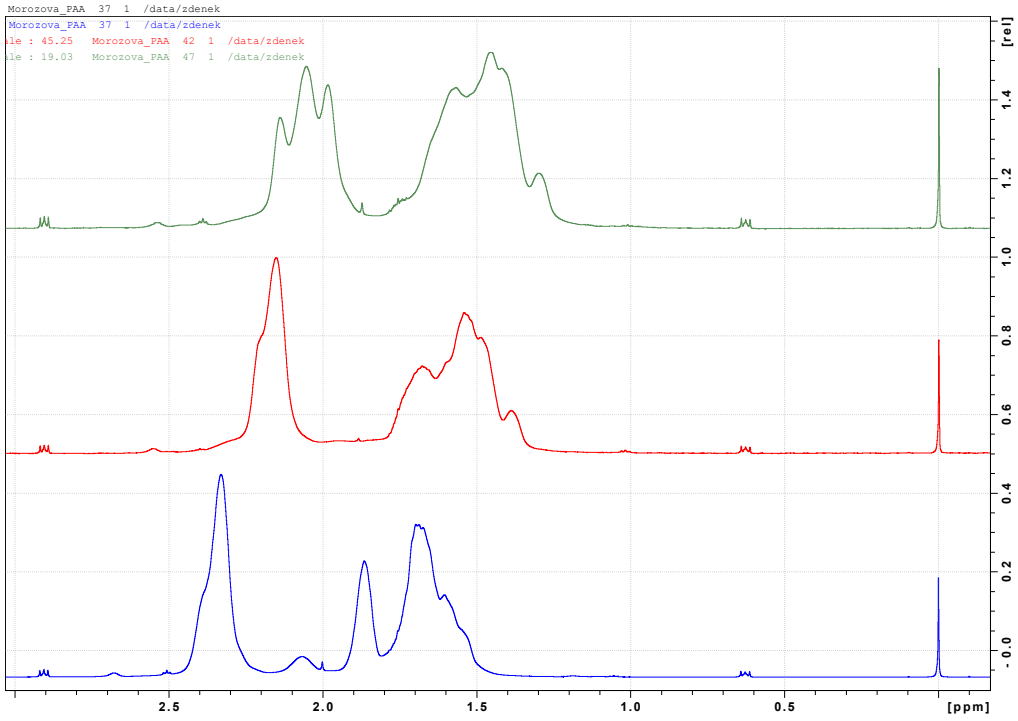

Figure 7: ^{1}H spectra of 0.4M solutions of PAA at different degrees of ionization: blue - 0.207; red - 0.725; green - 0.996

3.2.2 ^{13}C spectra

Figure 8 shows the ^{13}C spectrum of 1.575M solution of PAA at degree of ionization 0.380. A prominent resonance near 180 ppm attributes to the carboxyl carbon of -COOH/-COO^- group, reflecting both protonated and deprotonated species under this conditions. Multiple peaks between 40 and 60 ppm correspond to the aliphatic carbons of polymer backbone.

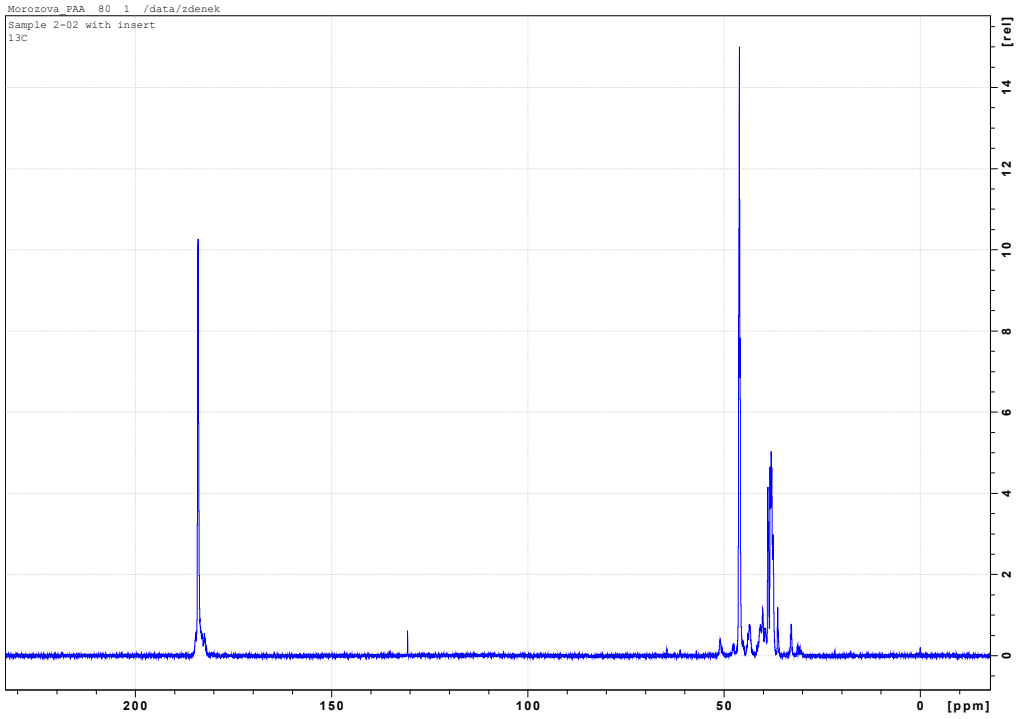

Figure 8: ^{13}C spectrum of 1.575M solution at ionization 0.380

The degree of ionization, α, was calculated based on the chemical shift changes of carboxyl group. To establish reference points, it was assumed that the sample without any addition of NaOH (initial pH) was non-ionized ($\alpha = 0.000$) and the sample prepared with large excess of NaOH was considered fully ionized ($\alpha = 1.000$). The degree of ionization for all other samples was then determined by linear interpolation of chemical shifts between these reference values.

Figure 9 presents the carboxylic region of ^{13}C spectra for 0.4M PAA solutions at different degrees of ionization. As ionization increases carboxyl signal undergoes downfield shift and broadening. At low ionization, a sharp peak at approximately 183 ppm represents a largely protonated environment. In partially ionized state, the signal broadens indicating dynamic equilibrium between -COOH and -COO$^-$ species. At high ionization, doubled peak arises due to conformational rearrangements.

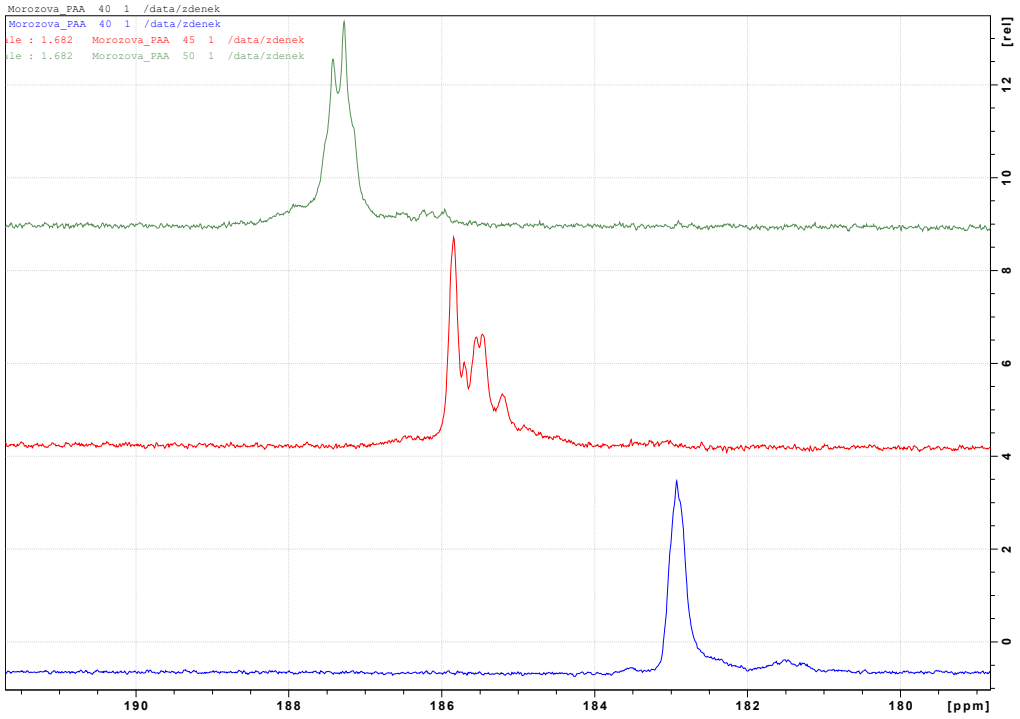

Figure 9: ^{13}C spectra of COOH group of 0.4M solutions of PAA at different degrees of ionization: blue - 0.207; red - 0.725; green - 0.996

3.2.3 DOSY

Figure 10 presents the signal intensity decay as a function of gradient strength. Experimental data were fitted using Eq. (12), which describes a bi-exponential decay model to account the presence of two diffusing components.

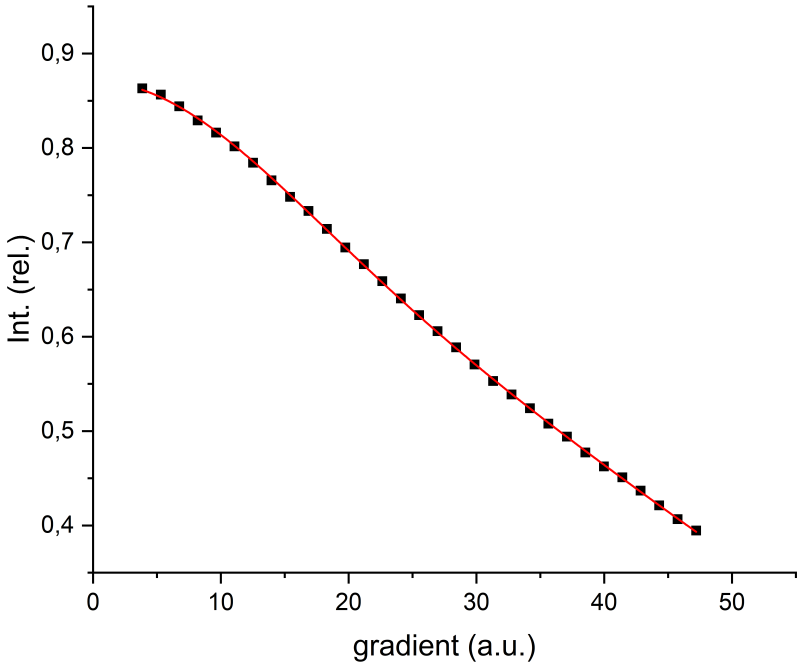

Figure 10: dependence of magnetic field's gradient on intensity of signal of 0.846M PAA solution at degree of ionization 0.529 fitted by Eq. (12)

Diffusion coefficients and relative contributions were obtained by fitting signal attenuation to a bi-exponential decay model using Origin. The results corresponding to the polymer sample shown in Figure 10 are summarized in Table 1 below.

D_1, m^2 s^{-1}	1.24×10^{-12}
D_2, m^2 s^{-1}	1.22×10^{-11}
a	79%
b	21%
R-Square	0.9999

Table 1: diffusion coefficients and relative contribution obtained from bi-exponential fitting. Results are given for sample from Fig. 12

Figure 11 represents the concentration behaviour of two translational diffusion coefficients D_1 and D_2 obtained from bi-exponential fitting of different polymer solutions at varying degrees of ionization. The x-axis represents polymer concentration on logarithmic scale. Different colours correspond to different ionization degrees, ranging from 0.0 (non-ionized) to 1.0 (fully ionized).

Across all ionization states, both diffusion coefficients decrease with increasing polymer

concentration. Notably, at low concentrations and low degrees of ionization, both diffusion coefficients are significantly higher, indicating minimal interchain association, resulting in higher chain mobility. At higher concentration, diffusion coefficients drop due to increased polymer-polymer interactions.

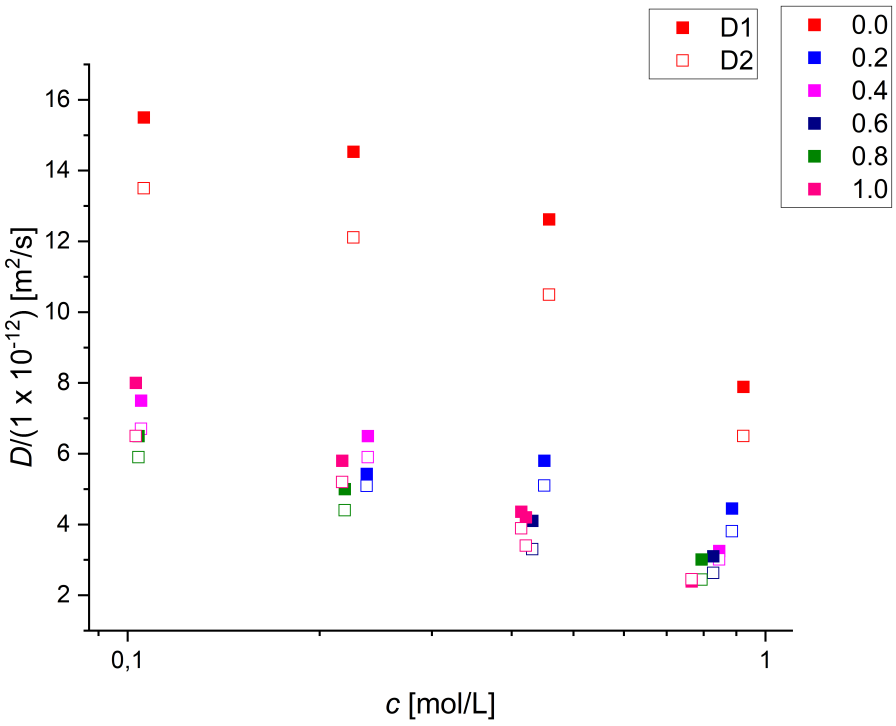

Figure 11: concentration dependence of two diffusion coefficients; colors indicate ionization degree: 0.0(red), 0.2(blue), 0.4(magenta), 0.6(navy), 0.8(green) and 1.0(pink); filled squares represent D_1, while opened - D_2

Figure 12 represents the concentration behaviour of two translational diffusion coefficients D_1 and D_2 in non-ionized state. The change in direction, indicated by dashed vertical line, corresponds with overlap concentration, which here equals to 0.4M.

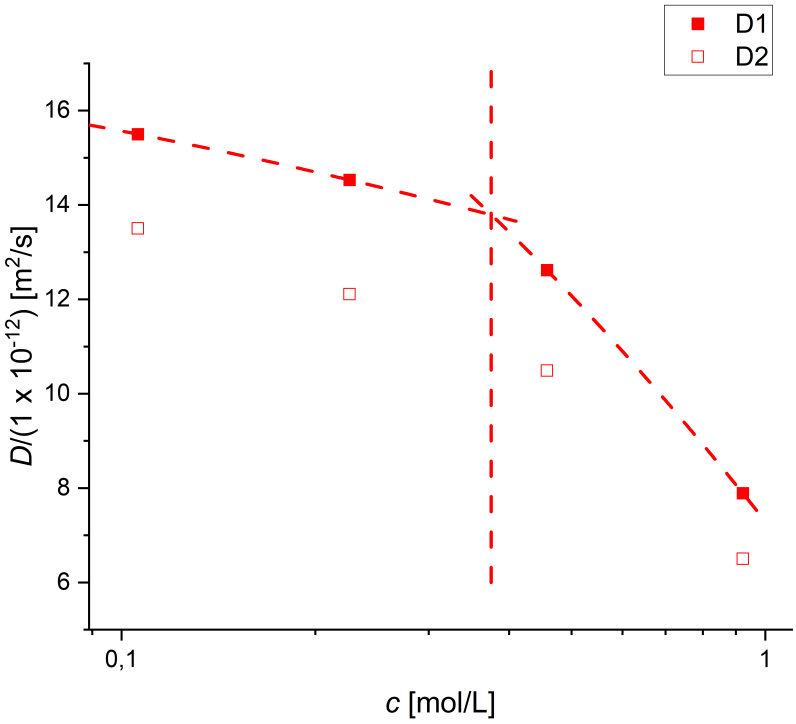

Figure 12: concentration dependence of two diffusion coefficients for non-ionized samples; filled squares represent D_1, while opened - D_2; dashed vertical line marks the transition between dilute and semi-dilute regimes

3.3 Titration

Each sample was prepared as follows. PAA was weighed directly into a titration flask in an amount that would give the desired concentration in a final volume of 2.5 mL. The exact mass of PAA was recorded, after which the precise volume of ultrapure water required to reach that concentration was calculated. This volume of water was then added gravimetrically and the actual PAA concentration was recalculated.

The degree of ionization α of PAA was calculated using following expression

$$\alpha = \frac{c_{\mathrm{Na^+}} + 10^{-\mathrm{pH}} - \frac{K_\mathrm{w}}{10^{-\mathrm{pH}}}}{c_{\mathrm{PAA}}}, \tag{13}$$

where $c_{\mathrm{Na^+}}$ is concentration of added sodium ions, c_{PAA} corresponds to total concentration of polymer and K_w is equilibrium constant for self-ionization reaction of water.

In subsequent experiments, c/c^* will be reported to enable better comparison with simulation results.

3.3.1 Dilute regime

Three different solutions were measured in dilute regime. Each figure shows the titration curve plotting degree od ionization, calculated using Equation (13), against pH - pK_a. In this thesis, pK_a value of acrylic acid, which equals 4.25 at 25°C, was used[28].

Figure 13 shows most dilute concentration measured. It was primarily chosen for setting up and validating the experimental method. The experimental data were fitted using Equation (8) for degrees of ionization from 0.0 to 0.83.

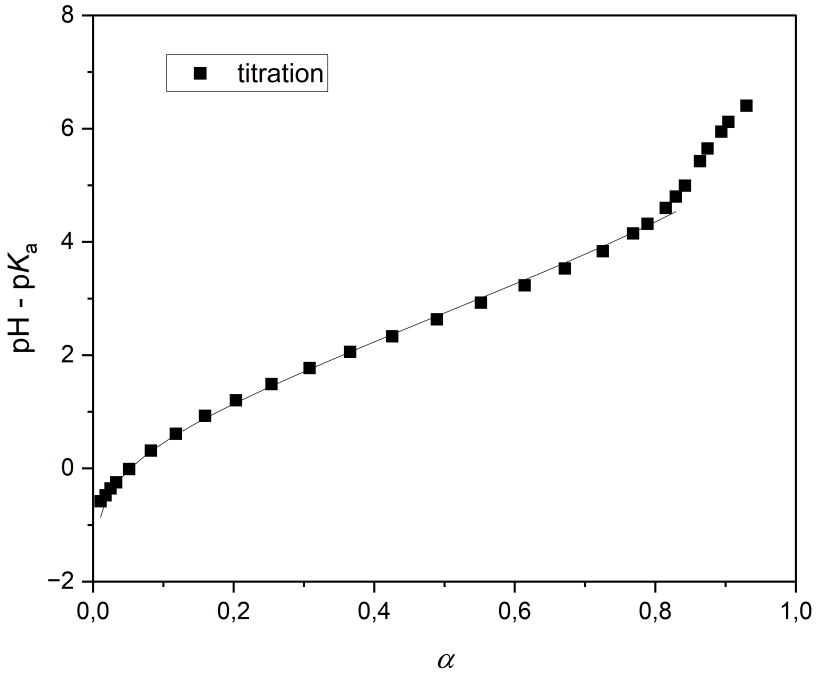

Figure 13: titration curve: dependence of α on pH - pK_a for $c/c^* = 5.33 \times 10^{-2}$

Table 2 presents the parameters obtained from fitting the titration curve corresponding to the sample shown in Fig. 13.

k	3.4
k_γ	27.2
R-Square	0.9999

Table 2: parameters obtained from fitting of titration curve. Results are given for sample from Fig. 13

Figure 14 shows intermediate dilute concentration measured compared to NMR results

and simulation[1] results. The experimental titration data were fitted using Equation (8) for degrees of ionization from 0.0 to 0.89.

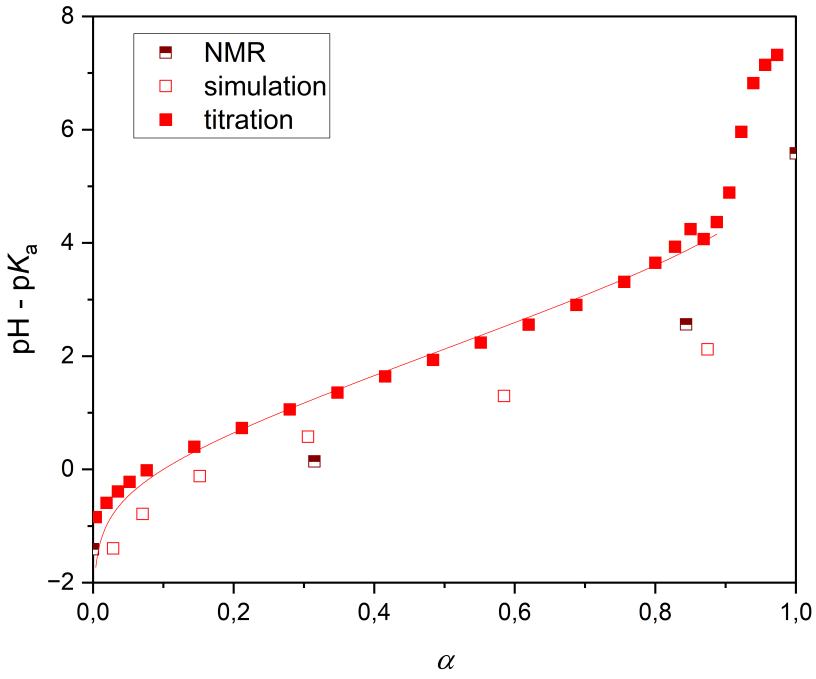

Figure 14: titration curve: dependence of α on pH - pK_a for $c/c^* = 2.66 \times 10^{-1}$

Table 3 presents the parameters obtained from fitting the titration curve corresponding to the sample shown in Fig. 14.

k	2.9
k_γ	9.7
R-Square	0.9998

Table 3: parameters obtained from fitting of titration curve. Results are given for sample from Fig. 14

Figure 15 shows highest concentration studied within dilute regime compared to NMR results. The experimental titration data were fitted using Equation (8) for degrees of ionization from 0.0 to 0.82.

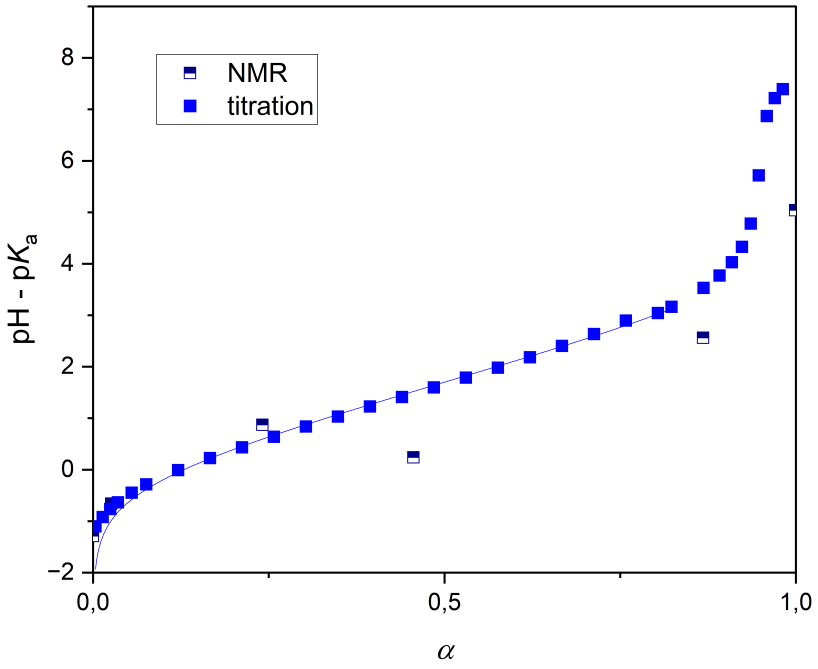

Figure 15: titration curve: dependence of α on pH - pK_a for $c/c^* = 5.56 \times 10^{-1}$

Table 4 presents the parameters obtained from fitting the titration curve corresponding to the sample shown in Fig. 15.

k	2.3
k_γ	6.3
R-Square	0.9999

Table 4: parameters obtained from fitting of titration curve. Results are given for sample from Fig. 15

3.3.2 Semi-dilute regime

Figure 16 shows lowest concentration studied within semi-dilute regime compared to NMR results.

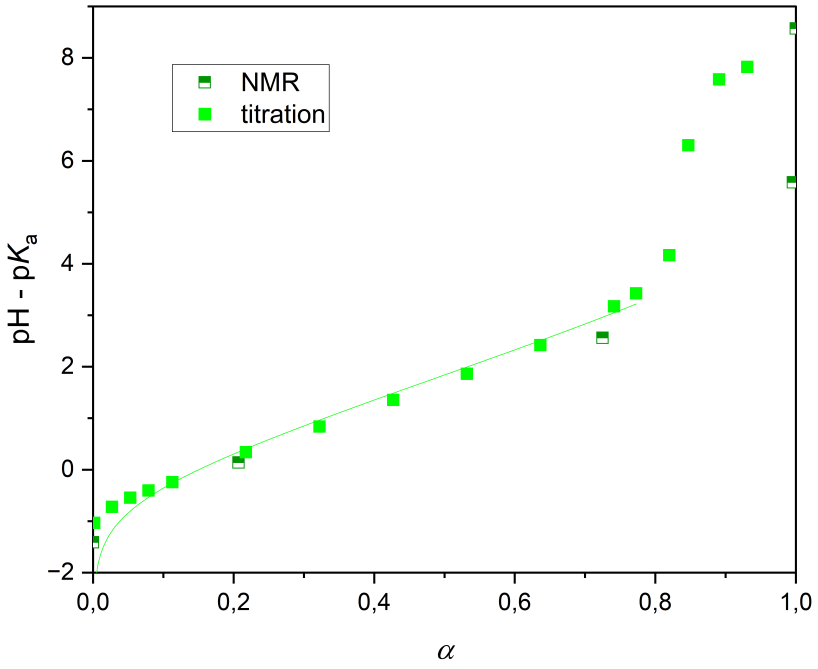

Figure 16: titration curve: dependence of α on pH - pK_a for $c/c^* = 1.05$

Table 5 presents the parameters obtained from fitting the titration curve corresponding to the sample shown in Fig. 16.

k	3.1
k_γ	2.9
R-Square	0.9997

Table 5: parameters obtained from fitting of titration curve. Results are given for sample from Fig. 16

Figure 17 shows intermediate concentration studied within semi-dilute regime compared to NMR results and simulation results.

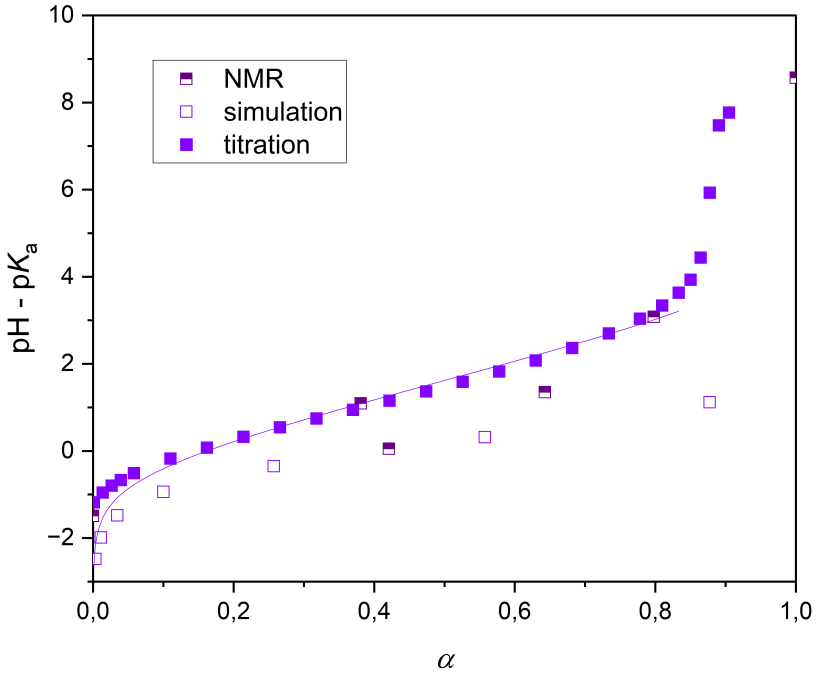

Figure 17: titration curve: dependence of α on pH - pK_a for $c/c^* = 2.21$

Table 6 presents the parameters obtained from fitting the titration curve corresponding to the sample shown in Fig. 17.

k	2.7
k_γ	2.5
R-Square	0.9996

Table 6: parameters obtained from fitting of titration curve. Results are given for sample from Fig. 17

Figure 18 shows highest concentration studied compared to NMR results.

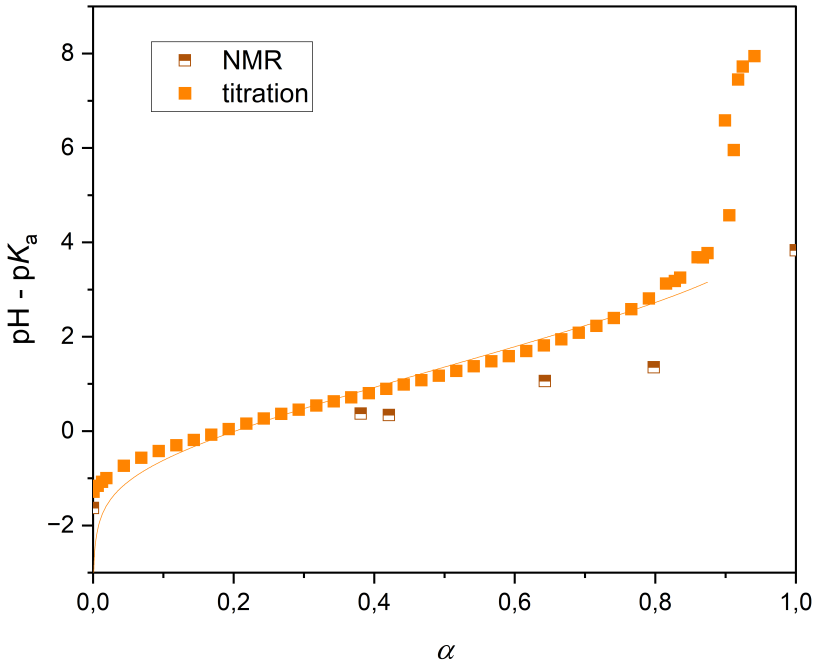

Figure 18: titration curve: dependence of α on pH - pK_a for $c/c^* = 4.62$

Table 7 presents the parameters obtained from fitting the titration curve corresponding to the sample shown in Fig. 18.

k	2.6
k_γ	0.6
R-Square	0.9994

Table 7: parameters obtained from fitting of titration curve. Results are given for sample from Fig. 18

Figure 19 shows comparison of all titration curves. The curves represent connected data points, and the legend indicates concentration as c/c^*.

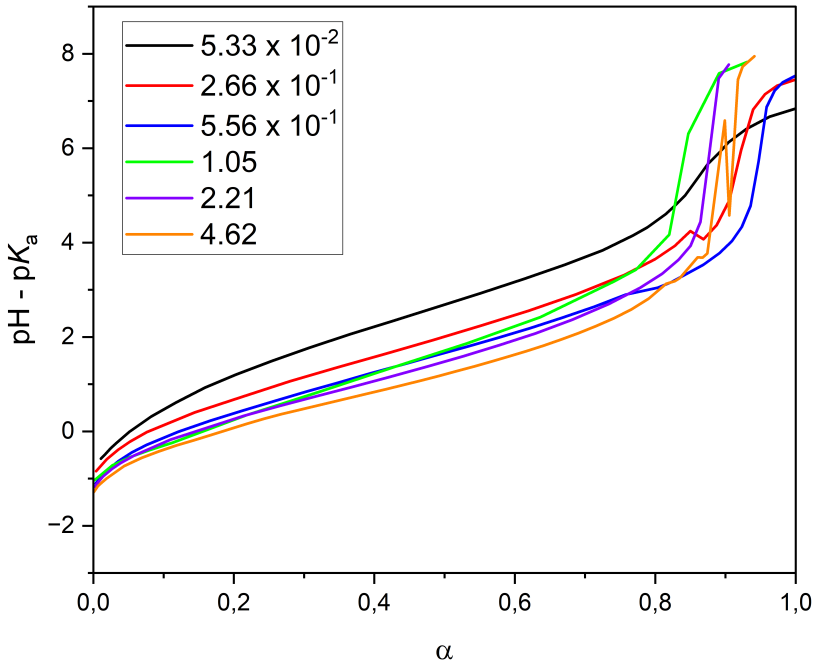

Figure 19: comparison of all titration curves: dependence of α on pH - pK_{a} for all concentrations

3.4 Discussion of results

One of the main challenges encountered in this study is the deviation between experimental titration data from both NMR data and theoretical predictions at high degrees of ionization, from approximately $\alpha \approx 0.8$. A key factor behind this deviation can be electrostatic repulsion that develops along the polymer backbone as more carboxyl groups ionize. In the highly charged state, the polymer chains can adopt collapsed conformations, in which deprotonated carboxyl groups are oriented toward the outer surface, while protonated groups remain shielded in the interior of the polymer coil. This structural organization creates a barrier to diffusion, limiting the accessibility of Na^+. As a result, even though titration continues, some carboxyl groups remain unreacted, leading to an underestimation of the degree of ionization.

From Figure 19 it is very clear that as the concentration increases, the titration curve moves downward. This trend reflects the influence of increased polymer concentration on the ionization behaviour of polyacrylic acid. However, at $c/c^* = 1.05$, the titration

curve shifts slightly upward. This behaviour likely corresponds to the transition between dilute and semi-dilute regimes. From this point onward, with increasing concentration the downward trend continues.

Another important aspect are values of k_γ, constant which accounts activity correction due to non-ideal behaviour. The results indicate that as polymer concentration increases, k_γ decreases, suggesting that the non-ideality diminishes at higher concentrations. This situation may seem counterintuitive, as higher concentrations often associates with stronger ion-ion interactions. The observed behaviour of weak polyelectrolyte is more complex then initially expected. This complexity is likely influenced, to some extent, by changes in solutions viscosity.

Another significant issue appears to be incomplete equilibrium during titration at high ionization. As polymer becomes charged, diffusion slows down and conformational changes take longer. Although the titrator may detect almost stable pH reading, the polymer system may not have reached full equilibrium on a microscopic level. In contrast, in NMR all samples were prepared in advance to ensure that complete equilibrium was reached before measurement.

A further complication arose from changing viscosity in highly ionized solutions [29]. This increase in viscosity can hinder molecular mobility, slowing down the diffusion processes and potentially preventing system from reaching equilibrium during titration experiments.

3.5 Study limitations and future perspectives

While this study provides valuable insights into the ionization behaviour of polyacrylic acid in the semi-dilute regime, several limitations should be acknowledged, as they are also represent opportunities for future research.

A key area for improvement lies in ensuring full equilibrium during titration, particularly at high degrees of ionization. Extending minimal equilibration times between titration steps could mitigate this issue and improve the reliability of titration data.

Another important limitation is the lack of measuring solutions viscosities as it could provide deeper understanding of the macroscopic changes associated with chain overlap. Similarly, incorporating Dynamic Light Scattering would allow to monitor hydrodynamic

radius in response to changes in ionic strength and pH.

Sample quality is also a critical factor. Gel Permeation Chromatography could be employed in future studies to control molecular weight distributions, to ensure reproducibility of experiments.

Finally, although DOSY was employed to determine the overlap concentration, further data - especially for ionized samples - would help to understand the diffusion behaviour across different regimes in ionized state.

4 Conclusion

DOSY NMR experiment was performed to investigate the diffusion behaviour of polyacrylic acid. Bi-exponential fitting revealed the presence of two distinct diffusion coefficients. Both diffusion coefficients decreased with increasing concentration, reflecting increasing solution viscosity. Ionization was found to significantly influence diffusion behaviour.

Overlap concentration was determined using DOSY NMR experiments, which provided diffusion coefficients across a range of polymer concentrations. In non-ionized solutions, a clear change of slope at concentration 0.4M was observed, indicating transition from the dilute to the semi-dilute regime.

For defined degrees of ionization at each concentration, the theoretical model demonstrates excellent agreement with experimental data. The model effectively captures the underlying physicochemical processes, the influence of ionic strength and electrostatic interactions.

However, the model could not be reliably tested at high degrees of ionization due to unreliable experimental results. Specifically, the system's equilibrium was established too slowly for the titrator to detect accurately, leading to untrustworthy results. Additionally, structural rearrangements may occur with the polymer forming compact coil-like structures, which shields $-COOH$ groups from NaOH, further contributing to incomplete deprotonation.

References

[1] Nová, L.; Stěpánek, M.; Morozova, I.; Tošner, Z.; Uhlík, F. Ionization and chain size of weak polyelectrolytes in semidilute regime. *Submitted to Macromolecules* **2025**,

[2] Griehl, W.; Ruestem, D. Nylon-12-Preparation, Properties, and Applications. *Industrial amp; Engineering Chemistry* **1970**, *62*, 16–22.

[3] Kim, D.; Kim, F. S. Materials Chemistry, Device Engineering, and Promising Applications of Polymer Transistors. *Chemistry of Materials* **2021**, *33*, 7572–7594.

[4] Rahman, C. V.; Saeed, A.; White, L. J.; Gould, T. W. A.; Kirby, G. T. S.; Sawkins, M. J.; Alexander, C.; Rose, F. R. A. J.; Shakesheff, K. M. Chemistry of Polymer and Ceramic-Based Injectable Scaffolds and Their Applications in Regenerative Medicine. *Chemistry of Materials* **2011**, *24*, 781–795.

[5] Sedláček, O.; Černoch, P.; Kučka, J.; Konefal, R.; Štěpánek, P.; Vetrík, M.; Lodge, T. P.; Hrubý, M. Thermoresponsive Polymers for Nuclear Medicine: Which Polymer Is the Best? *Langmuir* **2016**, *32*, 6115–6122.

[6] Rubinstein, M.; Colby, R. H. *Polymer Physics*; OUP Oxford, 2003.

[7] Laguecir, A.; Ulrich, S.; Labille, J.; Fatin-Rouge, N.; Stoll, S.; Buffle, J. Size and pH effect on electrical and conformational behavior of poly(acrylic acid): Simulation and experiment. *European Polymer Journal* **2006**, *42*, 1135–1144.

[8] Doi, M.; Edwards, S. F.; Edwards, S. F. *The Theory of Polymer Dynamics*; Oxford University Press, 1988.

[9] de Gennes, P. *Scaling concepts in polymer physics*; Cornell Univ. Pr.: Ithaca [u.a.], 1979; p 324 S.

[10] Ilnytskyi; Holovatch How does the scaling for the polymer chain in the dissipative particle dynamics hold? *Condensed Matter Physics* **2007**, *10*, 539.

[11] Matsumoto, A.; Zhang, C.; Scheffold, F.; Shen, A. Q. Microrheological Approach for Probing the Entanglement Properties of Polyelectrolyte Solutions. *ACS Macro Letters* **2021**, *11*, 84–90.

[12] Aoki, K.; Sugawara-Narutaki, A.; Takahashi, R. Polymeric Sol–Gel Transition with the Diverging Correlation Length Verified by Small-Angle X-ray Scattering. *The Journal of Physical Chemistry Letters* **2023**, *14*, 10396–10401.

[13] Kol, R.; Nachtergaele, P.; De Somer, T.; D'hooge, D. R.; Achilias, D. S.; De Meester, S. Toward More Universal Prediction of Polymer Solution Viscosity for Solvent-Based Recycling. *Industrial amp; Engineering Chemistry Research* **2022**, *61*, 10999–11011.

[14] Sakdaphetsiri, K.; Teanphonkrang, S.; Schulte, A. Cheap and Sustainable Biosensor Fabrication by Enzyme Immobilization in Commercial Polyacrylic Acid/Carbon Nanotube Films. *ACS Omega* **2022**, *7*, 19347–19354.

[15] Sideridou, I. D.; Achilias, D. S.; Karava, O. Reactivity of Benzoyl Peroxide/Amine

System as an Initiator for the Free Radical Polymerization of Dental and Orthopaedic Dimethacrylate Monomers: Effect of the Amine and Monomer Chemical Structure. *Macromolecules* **2006**, *39*, 2072–2080.

[16] Bunyakan, C.; Hunkeler, D. Precipitation polymerization of acrylic acid in toluene. I: synthesis, characterization and kinetics. *Polymer (Guildf.)* **1999**, *40*, 6213–6224.

[17] McNeill, I.; Sadeghi, S. Thermal stability and degradation mechanisms of poly(acrylic acid) and its salts: Part 1—Poly(acrylic acid). *Polymer Degradation and Stability* **1990**, *29*, 233–246.

[18] Rizwan, M.; Yahya, R.; Hassan, A.; Yar, M.; Azzahari, A.; Selvanathan, V.; Sonsudin, F.; Abouloula, C. pH Sensitive Hydrogels in Drug Delivery: Brief History, Properties, Swelling, and Release Mechanism, Material Selection and Applications. *Polymers* **2017**, *9*, 137.

[19] Skoog, D. A.; West, D. M.; Holler, F. J.; Crouch, S. R. *Fundamentals of Analytical Chemistry*; 2021.

[20] Volmer, D. A.; Curbani, L.; Parker, T. A.; Garcia, J.; Schultz, L. D.; Borges, E. M. Determination of Titratable Acidity in Wine Using Potentiometric, Conductometric, and Photometric Methods. *Journal of Chemical Education* **2017**, *94*, 1296–1302.

[21] Hore, P. J. *Nuclear Magnetic Resonance*; Oxford University Press, USA, 2015.

[22] Atkins, P. W.; De Paula, J.; Keeler, J. *Atkins' Physical Chemistry*; Oxford University Press, 2023.

[23] Günther, H. *NMR Spectroscopy*; John Wiley Sons, 2013.

[24] Hore, P. J.; Jones, J. A.; Wimperis, S. *NMR*; Oxford University Press, USA, 2015.

[25] Johnson, C., Jr. Diffusion ordered nuclear magnetic resonance spectroscopy: principles and applications. *Progress in Nuclear Magnetic Resonance Spectroscopy* **1999**, *34*, 203–256.

[26] Jerschow, A.; Müller, N. Suppression of Convection Artifacts in Stimulated-Echo Diffusion Experiments. Double-Stimulated-Echo Experiments. *Journal of Magnetic Resonance* **1997**, *125*, 372–375.

[27] Longsworth, L. G. THE MUTUAL DIFFUSION OF LIGHT AND HEAVY WATER. *The Journal of Physical Chemistry* **1960**, *64*, 1914–1917.

[28] Riddick, J. A.; Bunger, W. B.; Sakano, T. K. *Techniques of Chemistry 4th ed., Volume II. Organic Solvents*; John Wiley and Sons: New York, NY, 1985.

[29] Dou, S.; Colby, R. H. Charge density effects in salt-free polyelectrolyte solution rheology. *Journal of Polymer Science Part B: Polymer Physics* **2006**, *44*, 2001–2013.